

## Time-resolved studies of single semiconductor quantum dots

Valéry Zwiller,\* Mats-Erik Pistol, Dan Hessman, Rolf Cederström, Werner Seifert, and Lars Samuelson  
*Solid State Physics, Lund University, Box 118, S-22100 Lund, Sweden*  
 (Received 4 February 1998; revised manuscript received 10 September 1998)

We present time-resolved optical studies of single self-assembled quantum dots. The dots were obtained by Stranski-Krastanow growth of InP on  $\text{Ga}_{0.5}\text{In}_{0.5}\text{P}$ . A selective technique based on etching after electron-beam lithography, combined with the use of an optical microscope to enhance the spatial resolution of a time-resolved photoluminescence system, enabled the observation of single quantum dots. The emission linewidth of a single InP dot is observed to be around 3 meV. The evolution of the time-resolved photoluminescence spectra was studied as a function of excitation intensity. Under intense pulsed excitation the decay is no more a simple exponential due to feeding from higher energy levels, as a result of state filling. A four-level rate equation system is successfully used to model the results. [S0163-1829(99)06204-9]

### I. INTRODUCTION

Self-assembled quantum dots have been extensively studied.<sup>1</sup> However, crucial questions remain to be answered. The nature of the exciton-exciton,<sup>2</sup> exciton-photon, and exciton-phonon interactions requires further studies. Most of the studies performed to date have been done on a large number of dots with different characteristic sizes and emission energies. The study of single dots<sup>3-7</sup> yields more precise information. Time-resolved spectroscopy of single dots<sup>4,7</sup> is the ideal investigation tool to study the relaxation of excitons.

We have investigated the exciton recombination times in single self-assembled Stranski-Krastanov InP quantum dots embedded in  $\text{Ga}_{0.5}\text{In}_{0.5}\text{P}$ , grown by metal organic vapor phase epitaxy (MOVPE). The time-resolved study of single dots circumvents<sup>3,8</sup> the ambiguous broadening and position of the photoluminescence peaks due to statistical averaging inherent in the simultaneous study of a large ensemble of dots as reported so far.<sup>9-14</sup> Time-resolved photoluminescence was performed under different excitation intensities. The pulsed laser was exciting directly in the dots with an energy below the wetting layer energy. An exponential decay was observed under low excitation, while intense excitation induces a nonexponential decay. All the results presented here were obtained on two single quantum dots. A detailed macroscopic characterization of a similar sample was published elsewhere.<sup>8</sup> Results obtained on other quantum dots in the same sample are all in agreement with the presented results. The linewidths of different emission lines observed from single InP quantum dots is on the order of 3 meV, which is far broader than observed on single InAs dots<sup>6</sup>.

### II. EXPERIMENTAL METHODS

The sample was grown by low-pressure MOVPE in a horizontal rf-heated reactor, the details of which have been described earlier.<sup>10</sup> The growth started with the deposition of a 50-nm-thick GaAs buffer layer on a (100) GaAs substrate, which was followed by the growth of a 300-nm-thick  $\text{Ga}_{0.5}\text{In}_{0.5}\text{P}$  layer as the lower barrier. A short introduction of TMI produced the quantum dots which were then, after 12 s of growth interruption, capped by a  $\text{Ga}_{0.5}\text{In}_{0.5}\text{P}$  layer 300

nm thick. The typical shapes of these dots, grown at  $580^\circ\text{C}$ , are truncated pyramids with a hexagonal base of dimensions 40–60 nm and height 12–18 nm.<sup>15</sup>

The sample was patterned using electron-beam lithography. A 250-nm-thick PMMA layer was used as resist. The patterns consisted of arrays of disks of different sizes, ranging from 100 to 800 nm in diameter. After the lithography, etching was performed in a plasma etching system.<sup>16</sup> The mesas obtained were 10  $\mu\text{m}$  apart so that the exciting laser beam could easily be focused on only one mesa. Mesas containing single dots were identified by taking images of the structures under laser excitation through a tunable bandpass filter and the presence of single quantum dots was confirmed by PL spectra. Most single dots were found in mesas with a diameter of 400 nm.

Time-resolved PL measurements were obtained using a pulsed laser diode emitting 40-ps pulses at 1.899 eV with a  $10^6$  Hz repetition rate. The energy of this laser was lower than the absorption edge of the wetting layer (1.93 eV) and of the GaInP barrier (1.97 eV). Thus the carriers were directly generated in the dot, preventing any delay related to the capture of carriers from the barrier or from the wetting layer.<sup>14</sup> The detection system consisted of a streak camera with a time resolution of 15 ps and a 0.25-m monochromator. An additional cw argon ion laser emitting at 2.54 eV (488 nm) was used in some experiments, in conjunction with the pulsed laser. The luminescence was collected by an optical microscope with a numerical aperture of 0.5 and the laser excitation was focused on the targeted mesa with the same microscope. The sample was placed in a temperature-controlled cold finger He cryostat, with a temperature range of 3.5–300 K, offering good temperature stability on an hour time scale. Because of the very weak luminescence emanating from a single quantum dot, the spectra were obtained through several hours of integration. This micro-PL setup offers a spatial resolution of about 1.5  $\mu\text{m}$ .

### III. TIME-RESOLVED PHOTOLUMINESCENCE WITHOUT BACKGROUND EXCITATION

Figure 1(a) shows the time-resolved photoluminescence spectrum obtained from a single quantum dot (referred to as

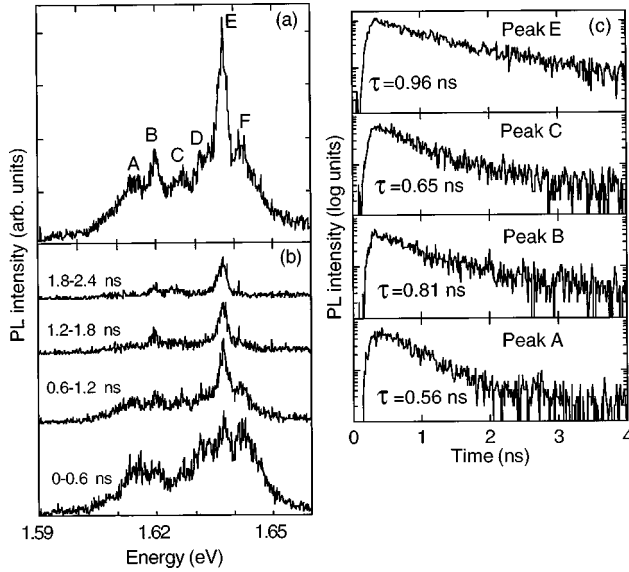


FIG. 1. (a) PL spectrum of a single InP dot (dot 1) taken at 7 K under low excitation. Six peaks are clearly distinguishable, referred to as A–F. (b) Time evolution of the spectra. (c) PL decays of peaks A, B, C, and E.

dot 1) at 7 K. The dot was excited with the pulsed laser diode only. The spectrum was obtained by integrating during 3 ns following the excitation. The spectra in Fig. 1(b) correspond to successive time-integrated windows 0.6 ns long. In the spectra, six peaks are distinguishable, A–F, from low to high energy, the lowest emission being at 1.615 eV and the highest being at 1.645 eV. We will refer to this never-vanishing set of peaks as the fundamental manifold.<sup>17,4</sup> The energy spacing between successive peaks in the fundamental manifold is about 6 meV. Peak E shows the strongest intensity; from Fig. 1(b) it is clearly seen that this higher intensity peak has the longest time constant: after 1.8 ns, peak E is the only peak clearly visible. Peak E also shows the narrowest line width of 3 meV [full width at half maximum (FWHM)]. Previous studies have shown that there are states at an energy which is higher than the fundamental manifold.<sup>4</sup> These higher-energy states can be observed both using state filling and by photoluminescence excitation spectroscopy.<sup>4</sup> The states in the fundamental manifold are, however, experimentally distinguished from higher-energy states by showing no sign of state filling under low excitation power density. Theoretical calculations, using six-band  $\mathbf{k}\cdot\mathbf{p}$  theory, in conjunction with the envelope function approximation,<sup>18</sup> as well as four-band calculations,<sup>19</sup> are in good agreement with photoluminescence results and indicate about 100 levels in the dot. The excitation in this experiment is directly into one of the excited states. Although we do not know the exact relaxation process, we do know that the relaxation from higher-energy states to states in the fundamental manifold is not very sensitive to the excitation energy.<sup>4</sup>

The time decay curves for different peaks are shown in Fig. 1(c). The decays were fitted with the formula

$$I(t) = \exp(-t/\tau),$$

where  $\tau$  is the time constant. The first 3.5 ns following the laser excitation were used for fitting. We estimate an uncer-

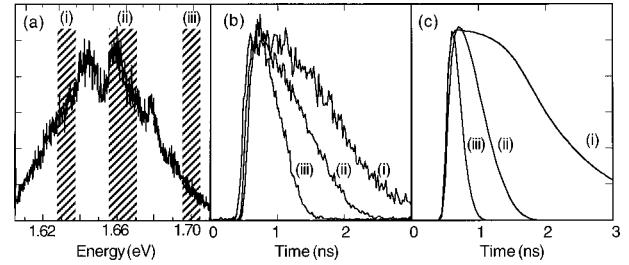


FIG. 2. (a) PL spectra (dot 2) taken under intense excitation. State filling is clearly seen; several peaks appear at higher energies. (b) shows the time evolution for energy regions (i), (ii), and (iii). The lowest-energy peak (i) shows a plateau before an exponential decay, while higher-energy regions do not exhibit this behavior. In (c) the simulated time evolution of the intensities is shown.

tainty of about 0.1 ns. Different peaks are found to have different time constants. The time constant of all the dots (about 25) that we have measured is around 0.6–1.0 ns. If the time constants were determined by a nonradiative channel, we would expect a larger spread in time constants, due to, e.g., the position of a nonradiative defect in the vicinity of the dot. We thus attribute the observed time constants to the intrinsic recombination time constants of these quantum dots. The intrinsic recombination time constant may be influenced by phonons, such as interface phonons and other types of phonons (for instance, localized to edges and corners), which we however consider to be native to the dots. The different intensities of the peaks observed cannot be explained by different transition probabilities, since at sufficiently low carrier density every electron-hole pair will eventually recombine. We instead attribute the intensity differences to state-dependent captures.

In Fig. 2 we present a photoluminescence spectrum from dot 2. At short delays we observe strong state filling, with new lines appearing at energies above 1.64 eV. The luminescence decay [Fig. 2(b)] is shown for different peaks. Initially a period of almost constant photoluminescence intensity is observed, under intense excitation for the low energy peaks. We attribute this to the fact that during this short time, the number of excitons cascading down from higher levels compensates the number of excitons recombining in the fundamental manifold levels.

If we compare our results with those in Ref. 7, we find strong similarities, despite the different material systems (strained InP quantum dots with sharp interfaces in our case versus quantum dots created by laser interdiffusion in the lattice matched AlGaAs/GaAs system). The sizes of the dots studied here are much smaller than those studied in Ref. 7. An experimental difference is that for the smallest dot studied in Ref. 7, effects of a slow relaxation were found, which we do not observe, demonstrating that the carrier relaxation mechanism is sensitive to the type of quantum dot and/or the material system.

#### IV. RATE EQUATION MODEL

To understand the nonexponential decay of low-energy peaks under strong excitation, we suggest a simple rate equation model.<sup>20,21</sup> In our model the excitons are captured by the

quantum dot in high-energy levels and then relax to lower levels. Relaxation to a lower level is only possible if the lower level is empty, due to the Pauli exclusion principle. In this model, we do not account for statistical fluctuations.<sup>22</sup> Although the charge carriers in a quantum dot cannot escape Coulomb effects, it is an oversimplification to use the term exciton if there is more than one electron-hole pair present in the quantum dot. We still use the term, since many-particle effects have been shown to be weak in this system<sup>4</sup> as well as in the InAs/GaAs system.<sup>6</sup>

This cascade mechanism<sup>23</sup> can be illustrated with a simple four-level rate equation in which excitons are allowed to relax from higher-energy levels and populate lower levels. The rise times of the photoluminescence peaks are short, faster than 100 ps. These experimentally observed short rise times imply fast relaxation time constants ( $\tau_{rel} \leq 100$  ps). Under low excitation, no luminescence from the higher states is detected, implying that the excitons cascade down to low energies before they recombine with a time constant  $\tau_{rec}$ . The recombination time constant is therefore much larger than the relaxation time constant ( $\tau_{rec}/\tau_{rel} \gg 1$ ).

The rate equations are

$$\begin{aligned} \frac{dn_1(t)}{dt} = & -\omega_{11}n_1(t) + \omega_{12}n_2(t)[1 - n_1(t)] \\ & + \omega_{13}n_3(t)[1 - n_1(t)] + \omega_{14}n_4(t)[1 - n_1(t)], \end{aligned} \quad (1)$$

$$\begin{aligned} \frac{dn_2(t)}{dt} = & -\omega_{22}n_2(t) - \omega_{12}n_2(t)[1 - n_1(t)] \\ & + \omega_{23}n_3(t)[1 - n_2(t)] + \omega_{24}n_4(t)[1 - n_2(t)], \end{aligned} \quad (2)$$

$$\begin{aligned} \frac{dn_3(t)}{dt} = & -\omega_{33}n_3(t) - \omega_{13}n_3(t)[1 - n_1(t)] \\ & - \omega_{23}n_3(t)[1 - n_2(t)] + \omega_{34}n_4(t)[1 - n_3(t)], \end{aligned} \quad (3)$$

$$\begin{aligned} \frac{dn_4(t)}{dt} = & -\omega_{44}n_4(t) - \omega_{14}n_4(t)[1 - n_1(t)] \\ & - \omega_{24}n_4(t)[1 - n_2(t)] - \omega_{34}n_4(t)[1 - n_3(t)] \\ & + g_{op}, \end{aligned} \quad (4)$$

$$g_{op} = 500e^{-450(t-1)^2}. \quad (5)$$

Here  $n_i$  is the population of level  $i$ ,  $\omega_{ij}$  is the transition probability from level  $j$  to level  $i$ , and  $g_{op}$  represents the creation of excitons by the laser in the high-energy levels. We assume that the probability for excitons to move up to higher-energy levels with time is always zero ( $\omega_{ij}=0$  for  $j < i$ ). We use  $\omega_{ii}=1/0.67$  ns<sup>-1</sup> and  $\omega_{ij}=1/0.03$  ns<sup>-1</sup> in our calculations (where  $\omega_{ii}$  is taken from the decay time without state filling). When the excitation is increased, the

population of higher-energy levels goes up; in our model  $n_4$  will increase. The expressions for  $g_{op}$  were chosen to approximate as closely as possible the shape of the laser pulse observed with the streak camera; it must, however, be kept in mind that  $g_{op}$  stands for the creation of excitons, not for the laser pulse itself.

Results obtained with our four-level model fit well to our experimental data, as can be seen by comparing Fig. 2(c) with Fig. 2(b). Higher-energy levels (above the fundamental manifold) have shorter time constants whereas low-energy peaks start with an almost constant intensity before decaying. This plateau indicates that the feeding from higher levels compensates the recombination in lower levels until the population of the higher levels vanishes.

The FWHM of the peaks that can be expected from Heisenberg's relation is  $\Delta E = \hbar/\Delta t$ ; taking  $\Delta t = 1$  ns, we obtain 1.5  $\mu$ eV. This theoretical value is far below the 3 meV observed experimentally (Fig. 1). The origin of these broad emission lines is not clear. It should be noted that the observed linewidth is larger than the spectral resolution of our system. For InAs quantum dots, the emission lines can be as sharp as 30  $\mu$ eV.<sup>6</sup> It should be noted, that the peaks do not get any sharper with time; 2 ns after the laser pulse [Fig. 1(b)], peak E still has 3 meV FWHM.

## V. STATE FILLING

In order to obtain some information on the recombination time constants of peaks at an energy higher than the fundamental manifold, a cw laser (emitting at 2.54 eV) was added to the pulsed beam. Thus there was at all times a certain population of carriers in the lower-energy states, which could be controlled by modifying the excitation power density of the cw laser. For sufficiently high excitation power density of the cw laser, the states in the fundamental manifold will be almost fully populated and we start to observe state filling.<sup>24</sup> A time-resolved measurement using the pulsed laser will then give a measure of the recombination time constant of states above the fundamental manifold, since the relaxation to lower-energy states is now hindered. Figure 3 shows time-integrated spectra for different excitation power densities of the cw laser denoted  $P_B$ , while the excitation power density of the pulsed laser is kept constant. For higher values of  $P_B$ , the spectra become broader and luminescence from higher-energy levels appear, due to state filling. The time evolution of the intensities has been fitted using the formula

$$I(t) = a + b \exp(-t/\tau), \quad (6)$$

and the values of  $\tau$  are given in Fig. 3. For peaks above the fundamental manifold we observe an increase in  $\tau$  (up to 0.36 ns) with increasing  $P_B$ , in agreement with expectations. In Fig. 4 we show the results of the rate-equation model, where we have used the same parameters as in Sec. V. The calculated time evolution has also been fitted using Eq. (6). Theoretically we also find an increase of  $\tau$  for peaks above the fundamental manifold for increasing  $P_B$ , in agreement with the experiments. For peaks belonging to the fundamen-

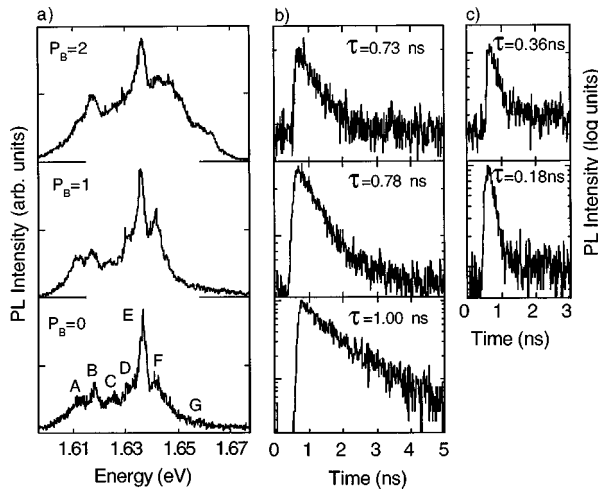


FIG. 3. Observing intense state filling (in dot 1) by the addition of a continuous-wave Ar<sup>+</sup> laser in addition to the pulsed laser diode. The PL spectra (a) were normalized,  $P_B$  is the excitation power density of the cw laser. Decay profiles are presented for both peaks E and G, shown in (b) and (c), respectively. Peak G only appears at higher excitations under intense state filling conditions. The time constants of peak G are shorter than the time constants of peak E.

tal manifold, no changes are observed, which does not agree with experiment. We nevertheless consider the agreement with experiment to be good, especially since we did not adjust the parameters of the model. We conclude from this experiment that the recombination time constant of peaks above the fundamental manifold is about 1 ns.

## VI. CONCLUSIONS

We have performed time-resolved photoluminescence studies on single InP quantum dots grown by metal organic vapor phase epitaxy on Ga<sub>0.5</sub>In<sub>0.5</sub>P. A four level rate equa-

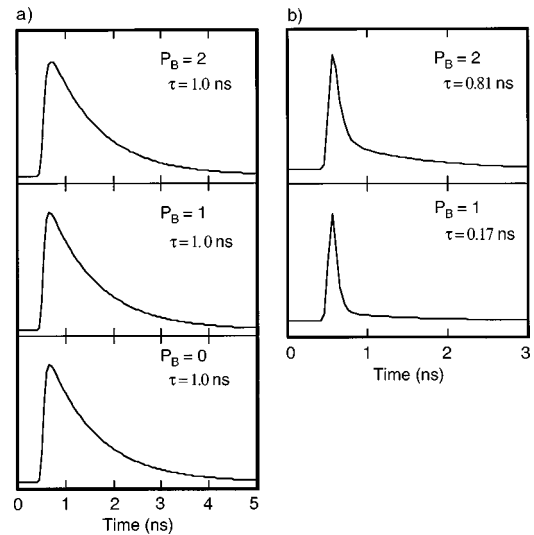


FIG. 4. Results of the rate-equation model, taking background excitation into account. Column (a) shows the time evolution of fundamental manifold peaks with increasing background excitation intensity. Column (b) shows the time evolution of state filled levels. The time constants are indicated in the figure.

tion model was found adequate to explain the experiments, using a recombination time constant of about 1 ns and a relaxation time constant of about 30 ps.

## ACKNOWLEDGMENTS

Ivan Maximov is acknowledged for processing of the sample. Carl-Olof Alamladh is thanked for critical discussions. We thank Bernhard Kowalski and Pedro Castrillo for a critical reading of the manuscript and useful discussions. This work was performed within the Nanometer Structure Consortium in Lund, Sweden, and was supported by NFR, TFR, NUTEK, and SSF.

\*Electronic address: Valery.Zwiller@ftf.lth.se

<sup>1</sup>W. Seifert, N. Carlsson, M. Miller, M.-E. Pistol, L. Samuelson, and L. R. Wallenberg, *Prog. Cryst. Growth Charact. Mater.* **33**, 423 (1996).

<sup>2</sup>J. Shah, *Ultrafast Spectroscopy of Semiconductors and Semiconductor Nanostructures*, Springer Series in Solid State Sciences Vol. 115 (Springer, New York, 1996).

<sup>3</sup>K. Brunner, U. Bockelmann, G. Abstreiter, M. Walther, G. Böhm, G. Tränkle, and G. Weimann, *Phys. Rev. Lett.* **69**, 3216 (1992).

<sup>4</sup>D. Hessman, P. Castrillo, M.-E. Pistol, C. Pryor, and L. Samuelson, *Appl. Phys. Lett.* **69**, 749 (1996).

<sup>5</sup>J.-Y. Marzin, J.-M. Gérard, A. Izraël, D. Barrier, and G. Bastard, *Phys. Rev. Lett.* **73**, 716 (1994).

<sup>6</sup>L. Landin, M. S. Miller, M.-E. Pistol, C. Pryor, and L. Samuelson, *Science* **280**, 262 (1998).

<sup>7</sup>U. Bockelmann, W. Heller, A. Filoramo, and Ph. Roussignol, *Phys. Rev. B* **55**, 4456 (1997).

<sup>8</sup>M.-E. Pistol, P. Castrillo, D. Hessman, S. Anand, N. Carlsson, W. Seifert, and L. Samuelson, *Solid-State Electron.* **40**, 357 (1996).

<sup>9</sup>H. Yu, S. Lycett, C. Roberts, and R. Murray, *Appl. Phys. Lett.* **69**, 4087 (1996).

<sup>10</sup>N. Carlsson, W. Seifert, A. Petersson, P. Castrillo, M.-E. Pistol,

and L. Samuelson, *Appl. Phys. Lett.* **65**, 3093 (1994).

<sup>11</sup>T. Kono, Y. Nagamune, M. Nishioka, and Y. Arakawa, *Superlattices Microstruct.* **17**, 73 (1995).

<sup>12</sup>A. Kurtenbach, W. W. Rühle, and K. Eberl, *Solid State Commun.* **96**, 265 (1995).

<sup>13</sup>U. Woggon and S. V. Gaponenko, *Phys. Status Solidi B* **189**, 285 (1995).

<sup>14</sup>T. Okuno, H. W. Ren, M. Sugisaki, K. Nishi, S. Sugou, and Y. Masumoto, *Phys. Rev. B* **57**, 1386 (1998).

<sup>15</sup>K. Georgson, N. Carlsson, L. Samuelson, W. Seifert, and L. R. Wallenberg, *Appl. Phys. Lett.* **67**, 2981 (1995).

<sup>16</sup>I. Maximov, A. Gustafsson, H.-C. Hansson, L. Samuelson, W. Seifert, and A. Wiedenohler, *J. Vac. Sci. Technol. B* **11**, 748 (1993).

<sup>17</sup>Previously, the term ‘‘ground manifold’’ was used. We here use the term fundamental manifold to avoid possible confusion with the ground state.

<sup>18</sup>C. Pryor, M.-E. Pistol, and L. Samuelson, *Phys. Rev. B* **56**, 10 404 (1997).

<sup>19</sup>S. Nomura, L. Samuelson, M.-E. Pistol, K. Uchida, N. Miura, T. Sugano, and Y. Aoyagi, *Appl. Phys. Lett.* **71**, 2316 (1997).

<sup>20</sup>B. Ohnesorge, M. Albrecht, J. Oshinowo, and A. Forchel, *Phys. Rev. B* **54**, 11 532 (1996).

- <sup>21</sup>S. Grosse, J. H. H. Sandmann, G. von Plessen, J. Feldman, H. Lipsanen, M. Sopanen, J. Tulkki, and J. Ahopelto, Phys. Rev. B **55**, 4473 (1997).
- <sup>22</sup>M. Grundmann and D. Bimberg, Phys. Rev. B **55**, 9740 (1997).
- <sup>23</sup>S. Raymond, S. Fafard, P. J. Poole, A. Wojs, P. Hawrylak, C. Gould, A. Sachrajda, S. Charbonneau, D. Leonard, R. Leon, P. M. Petroff, and J. L. Merz, Superlattices Microstruct. **21**, 541 (1997).
- <sup>24</sup>P. Castrillo, D. Hessman, M.-E. Pistol, S. Anand, N. Carlsson, W. Seifert, and L. Samuelson, Appl. Phys. Lett. **67**, 1905 (1995).